NASA/TM–2012-217571

Thermostructural Evaluation of Joggle Region on the Shuttle Orbiter's Wing Leading Edge

Sandra P. Walker and Jerry E. Warren
Langley Research Center, Hampton, Virginia

May 2012

NASA STI Program . . . in Profile

Since its founding, NASA has been dedicated to the advancement of aeronautics and space science. The NASA scientific and technical information (STI) program plays a key part in helping NASA maintain this important role.

The NASA STI program operates under the auspices of the Agency Chief Information Officer. It collects, organizes, provides for archiving, and disseminates NASA's STI. The NASA STI program provides access to the NASA Aeronautics and Space Database and its public interface, the NASA Technical Report Server, thus providing one of the largest collections of aeronautical and space science STI in the world. Results are published in both non-NASA channels and by NASA in the NASA STI Report Series, which includes the following report types:

- TECHNICAL PUBLICATION. Reports of completed research or a major significant phase of research that present the results of NASA Programs and include extensive data or theoretical analysis. Includes compilations of significant scientific and technical data and information deemed to be of continuing reference value. NASA counterpart of peer-reviewed formal professional papers, but having less stringent limitations on manuscript length and extent of graphic presentations.

- TECHNICAL MEMORANDUM. Scientific and technical findings that are preliminary or of specialized interest, e.g., quick release reports, working papers, and bibliographies that contain minimal annotation. Does not contain extensive analysis.

- CONTRACTOR REPORT. Scientific and technical findings by NASA-sponsored contractors and grantees.

- CONFERENCE PUBLICATION. Collected papers from scientific and technical conferences, symposia, seminars, or other meetings sponsored or co-sponsored by NASA.

- SPECIAL PUBLICATION. Scientific, technical, or historical information from NASA programs, projects, and missions, often concerned with subjects having substantial public interest.

- TECHNICAL TRANSLATION. English-language translations of foreign scientific and technical material pertinent to NASA's mission.

Specialized services also include organizing and publishing research results, distributing specialized research announcements and feeds, providing information desk and personal search support, and enabling data exchange services.

For more information about the NASA STI program, see the following:

- Access the NASA STI program home page at *http://www.sti.nasa.gov*

- E-mail your question to help@sti.nasa.gov

- Fax your question to the NASA STI Information Desk at 443-757-5803

- Phone the NASA STI Information Desk at 443-757-5802

- Write to:
  STI Information Desk
  NASA Center for AeroSpace Information
  7115 Standard Drive
  Hanover, MD 21076-1320

NASA/TM–2012-217571

Thermostructural Evaluation of Joggle Region on the Shuttle Orbiter's Wing Leading Edge

Sandra P. Walker and Jerry E. Warren
Langley Research Center, Hampton, Virginia

National Aeronautics and
Space Administration

Langley Research Center
Hampton, Virginia 23681-2199

May 2012

Available from:

NASA Center for AeroSpace Information
7115 Standard Drive
Hanover, MD 21076-1320
443-757-5802

Abstract

An investigation was initiated to determine the cause of coating spallation occurring on the Shuttle Orbiter's wing leading edge panels in the slip-side joggle region. The coating spallation events were observed, post flight, on differing panels on different missions. As part of the investigation, the high re-entry heating occurring on the joggles was considered here as a possible cause. Thus, a thermostructural evaluation was conducted to determine the detailed state-of-stress in the joggle region during re-entry and the feasibility of a laboratory test on a local joggle specimen to replicate this state-of-stress. A detailed three-dimensional finite element model of a panel slip-side joggle region was developed. Parametric and sensitivity studies revealed significant stresses occur in the joggle during peak heating. A critical interlaminar normal stress concentration was predicted in the substrate at the coating interface and was confined to the curved joggle region. Specifically, the high interlaminar normal stress is identified to be the cause for the occurrence of failure in the form of local subsurface material separation occurring in the slip-side joggle. The predicted critical stresses are coincident with material separations that had been observed with microscopy in joggle specimens obtained from flight panels.

Introduction

The reinforced carbon-carbon (RCC) leading edge panels, on the Shuttle Orbiter's wing, are coated with Silicon Carbide (SiC) to prevent oxidation at extreme temperatures associated with re-entry. An illustration showing the shuttle leading edge panels along the span of the wing, with a close-up of an individual panel and T-seal, is displayed in Fig. 1. The T-seals, located between the panels, are designed to prevent flow ingress during re-entry while allowing free thermal expansion of the panels across the span of the wing. The coating spallation events were observed post flight after two separate missions and on two different panels but both had occurred locally on the slip-side joggle region of the panels. A photograph showing a panel that experienced a spallation event is displayed in Fig. 2 along with a schematic illustrating the general region where spallation had occurred. Since the risk of loss of coating during re-entry could lead to a catastrophic burn through in the RCC substrate, the root cause investigation was initiated.

As part of the investigation, nondestructive evaluation (NDE) techniques were employed to assess panels post-flight and prior to future shuttle flights. The NDE effort revealed the existence of subsurface material separations located in the slip-side joggle region in the vicinity of the SiC coating interface with the RCC substrate on several panels (presented at the NASA STS-120 Flight Readiness Review in October 2007). Post-flight NDE images revealed a large region of concern on a RCC Panel 8 and the panel was removed for repair. During the refurbishment process, the coating in the joggle region was removed with a dental pick indicating the presence of subsurface structural degradation (Fig. 3).

Some RCC panels with NDE indications were cut up for microscopic evaluation. A micrograph showing the typical appearance of a subsurface material separation is displayed in Fig. 4. As illustrated, the separation in the joggle is contained mostly in the RCC substrate material near the outer-mold-line

(OML) SiC coating interface. The maximum material separation lengths measured were all limited to approximately 0.3-inches and were all confined to the curved portion of the joggle.

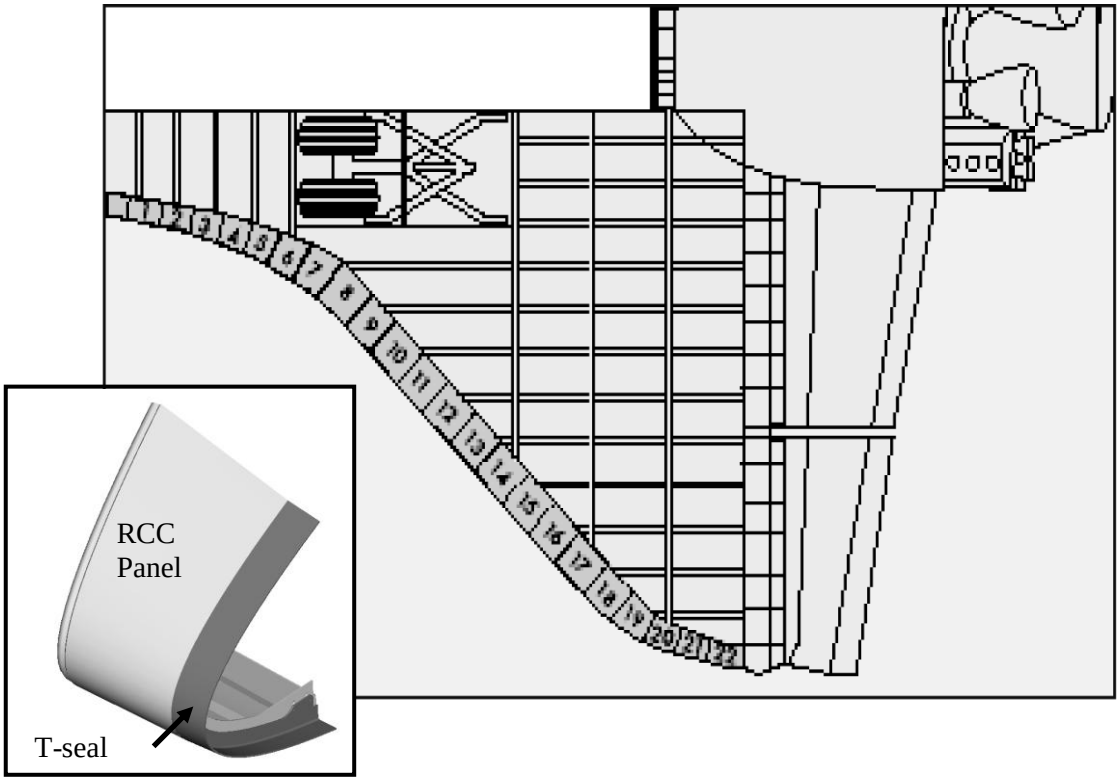

Fig. 1 Illustration of a bottom view of the Orbiter right wing with RCC leading edge panels identified by their respective numbers and of an individual panel with T-seal.

Prior to this root cause investigation, coated RCC had been treated as a homogeneous material system where smeared properties from testing coated RCC specimens were utilized for material properties in global analysis models (Ref. 1). With this approach, local thermal stresses that develop in the SiC coating and RCC substrate are not considered. A design drawing showing the actual plies in the joggle is displayed in Fig. 5. The acreage panel region is fabricated with 19 plies; a pad-up to 22 plies exists in the joggle region. The coating is formed by converting the outer surfaces of the carbon (0.02 to 0.04 inch) to SiC by a diffusion reaction (Ref. 2). During cool down, craze cracks form through the thickness of the coating due to thermal stresses (see Fig. 4). Coating acceptance criteria allows for surface craze cracks that do not exceed a width of 0.001 inch.

The current effort focuses on the root cause for the initiation of the subsurface material separations. The wing leading edge panels were designed to withstand both cyclic cold temperatures on-orbit and the extreme high heating associated with hypersonic re-entry into the Earth's atmosphere where temperatures near 2900^{o}F are experienced on some of the hottest panels (Panels 8-10). These thermal loading conditions are considered here to determine their significance on the detailed thermostructural response of the joggle region.

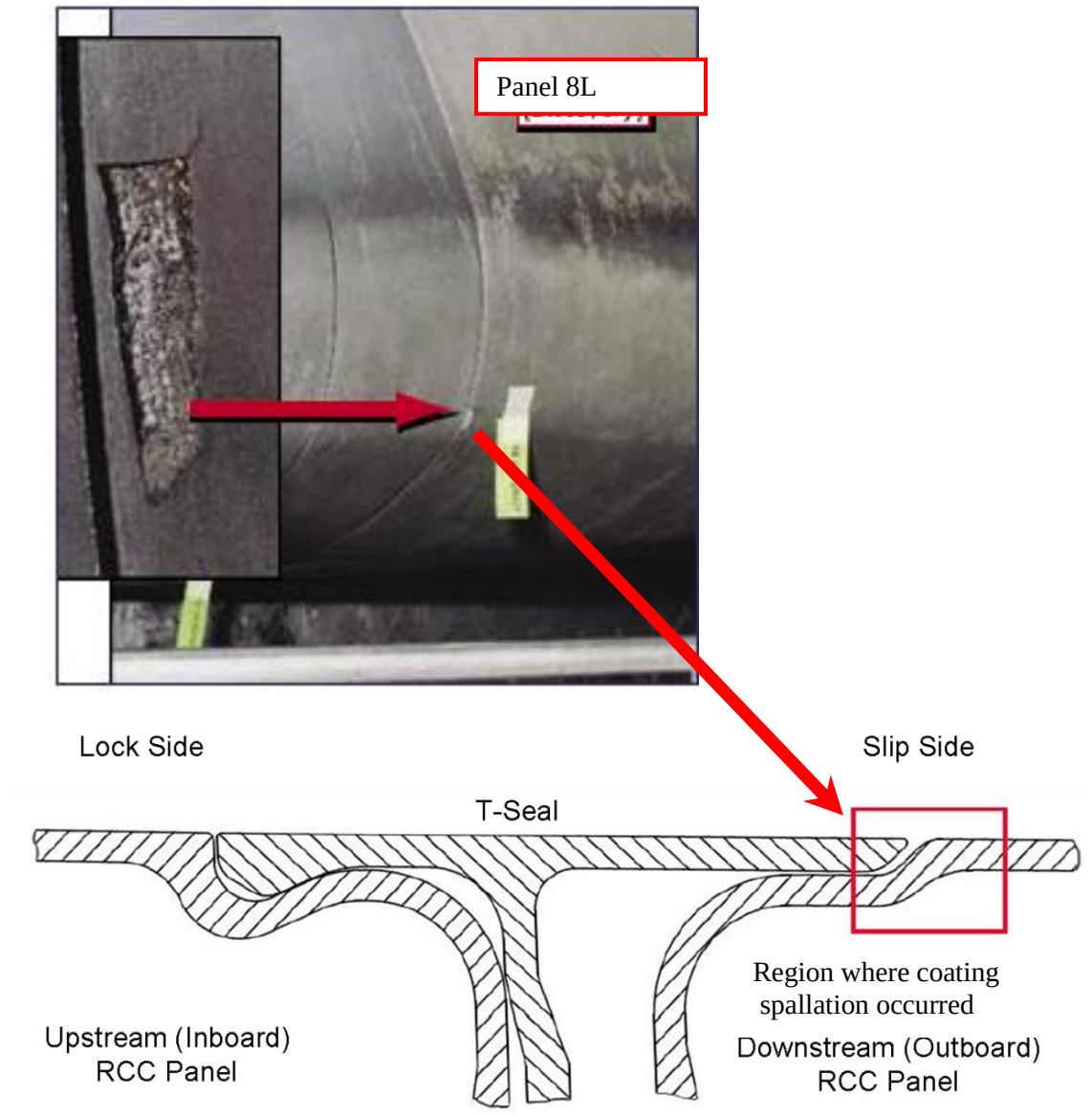

Fig. 2 Photograph of Panel 8L which had experienced coating spallation and schematic illustrating region where coating spallation events occurred.

In conjunction with this local joggle thermostructural analyses and evaluation effort, global shell analyses were performed using NASTRAN (Ref. 3) at Boeing Huntington Beach (by Okimo, D. and Ghahyasi, F. A., April 2008) to determine the global structural response of the panel when subject to the critical thermal load conditions. The NASTRAN models were delivered to NASA and evaluated in this effort. The global shell model was developed using smeared coated RCC properties, which computed insignificant magnitudes of stress in the joggle region at the time of peak heating and at the time when the peak spatial thermal gradients were predicted across the joggle span. Thus, the global panel contribution

to the thermostructural loads in the local joggle region was negligible and could not contribute significantly to failure initiation.

Fig. 3 Photograph of panel 8R showing slip-side joggle that had coating removed with dental pick during repair process.

The goal of the thermostructural analysis and evaluation effort (Ref. 4) presented in this paper was to determine if the thermal loading conditions experienced at the joggle during a Shuttle flight could initiate damage in the form of a material separation. In pursuit of this goal, the specific objectives of the local joggle thermostructural analysis included: developing a fundamental understanding of the significant parameters affecting the joggle response during re-entry, developing local finite element joggle models with sufficient detail to accurately predict local stress, determining the critical thermal loading conditions in the joggle region, and determining the optimal test conditions for initiating failure in a local joggle specimen. The local joggle test specimen would be cut from an existing wing leading edge panel to thermal cycle in a test facility and replicate the critical thermostructural state-of-stress expected during a mission cycle. Consequently parametric and sensitivity studies are performed to determine the specimen size, the required thermal load, and if additional mechanical restraints or loads are required in the test. Finally, failure theory is applied in evaluating the finite element analysis results, and the analysis predictions are compared to concurrently obtained test results to make an assessment of root cause.

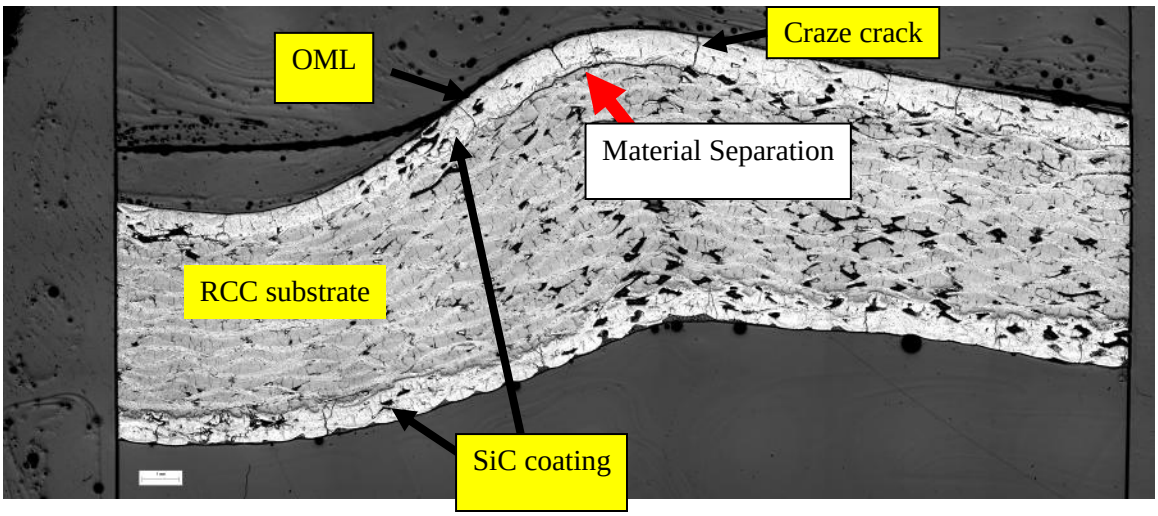

Fig. 4 Typical microscopic image of material separation associated with an NDE indication.

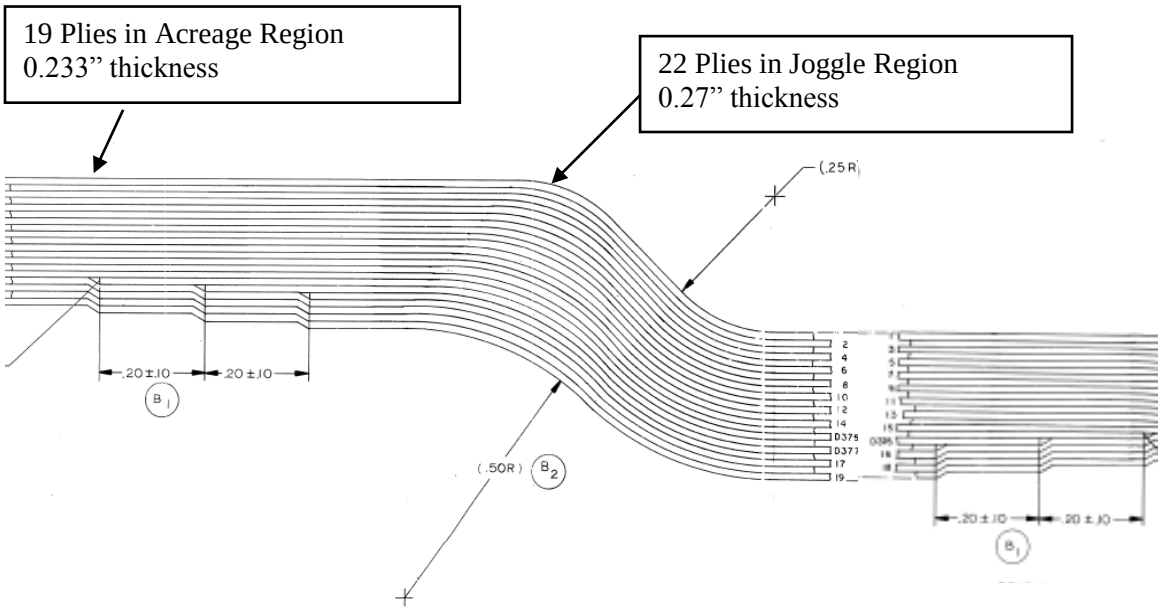

Fig. 5 Joggle design drawing showing pad-up from 19 to 22 plies in joggle.

Analytical Evaluation of Thermal Stress

A simplifying approximation of a plane stress model under uniform thermal load, as illustrated in Fig.

6, is utilized to develop a fundamental understanding on the significant parameters affecting thermal stress in the coating and substrate material system. The following assumptions are incorporated:

1) Isotropic material properties

2) Plane stress $\sigma_z = 0$ (thin plate)

3) $\sigma = \sigma_x = \sigma_y$ (uniform thermal load)

4) Negligible shear effects

with which the stress-strain relation for each material reduces to

$$\sigma_i = \frac{E_i}{1-\nu_i}\left[\varepsilon - \alpha_i \Delta T\right] \qquad i = 1,2 \tag{1}$$

where σ is stress, ε is strain, E is the modulus of elasticity, ν is the Poisson ratio, α is the coefficient of thermal expansion, and ΔT is the applied thermal load. The thermal load is the change in temperature

$$\Delta T = T - Tref \tag{2}$$

where T is the operating temperature and Tref is the stress free temperature (SFT) of the material system. When considering equilibrium of the material system, the sum of the in-plane forces reduces to

$$2\sigma_1 t_1 + \sigma_2 t_2 = 0 \tag{3}$$

where t is the thickness of each material in the composite. Substituting Eq. (1) into Eq. (3) and solving for the strain,

$$\varepsilon = \frac{\left[\frac{2E_1 t_1 \alpha_1}{1-\nu_1} + \frac{E_2 t_2 \alpha_2}{1-\nu_2}\right]\Delta T}{\frac{2E_1 t_1}{1-\nu_1} + \frac{E_2 t_2}{1-\nu_2}}, \tag{4}$$

which can be substituted into Eq. (1) to provide a closed-form solution for the stress in the coating or substrate. Similar methodology has been followed in predicting stresses in coated metals (Ref. 5). Using simplified isotropic properties for an applied operating temperature of 2900°F, which is near the peak temperature observed on a RCC panel, the ratio of stress to the average ultimate strength, F, in the coating is displayed graphically in Fig. 6 for two RCC thicknesses, while the coating thickness is constant. These equations reveal the composite thickness as an important parameter affecting thermal stress and more importantly the high sensitivity of stress to the SFT.

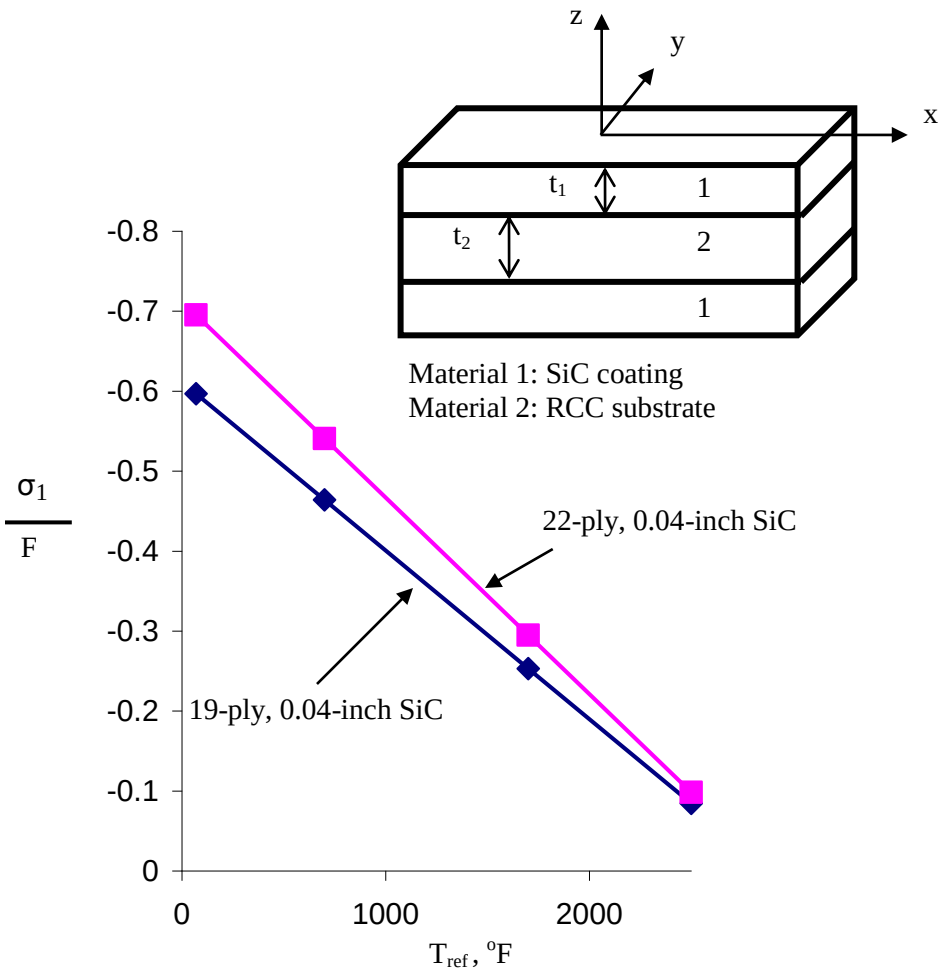

Fig. 6 Closed-form solution for thermal stress in SiC coating under uniform thermal load of 2900°F.

Stress Free Temperature

Further understanding on what is the SFT of the material system is required to predict accurately stresses in the material system when subject to thermal loading. Prior to this investigation there was no documented data on the SFT of the SiC coated RCC material system. The SiC surfaces of the panels are covered with craze cracks that occurred during panel fabrication. Hence, to get a first estimate on the SFT, the assumption was made that stresses only incur in the coating when the craze cracks close. The temperature when the cracks close is predicted assuming free thermal expansion of the coating from room temperature as follows

$$\varepsilon = \alpha \Delta T, \quad \text{where } \varepsilon = \frac{\delta}{L} \tag{5}$$

Using an average coating island length of L = 0.25-inch and crack closing width of δ = 0.001-inch, the temperature when cracks close is predicted to be about 1400^{o}F. This approach neglects residual stresses in SiC coating and RCC substrate that can accumulate between the actual SFT and the temperature that cracks close and also the restraint the RCC substrate imposes on free thermal expansion of the coating. This would not be a conservative approach if the actual SFT is less than the temperature when cracks close.

To understand the significance of stress that can develop in the coating islands when subject to a temperature change, a three-dimensional model of a coating island bonded to an RCC substrate was created as shown in Fig. 7. The stresses that result when subject to a temperature change of ΔT = 300^{o}F are also displayed in Fig. 7. Clearly, although the normal stresses at the free-edges are zero in the coating islands while the cracks remain opened, appreciable stresses can develop in the center of a coating island. Thus, average residual stresses in coating islands that exist prior to cracks closing during re-heating may be a significant contribution in predictions of stresses during peak heating.

The fabrication process is considered to formulate a more fundamental understanding of the SFT. A conceptual model for the determination of the SFT is hypothesized as illustrated graphically in Fig. 8. In the fabrication process, the RCC is heated to 3000^{o}F where RCC is converted to SiC. Initially the stress free temperature would be 3000^{o}F. During cooling, thermal stress builds up in the materials with differing material properties (Blue line). When the coating stresses reach the ultimate strength of the coating, craze cracks form and some stress is relieved (Green lines). Some residual stress remains in the newly formed coating islands between the craze cracks. As the material continues to cool, the process of cracking is repeated. Finally, when the material system is re-heated during re-entry (Red line), the coating initially has a residual tensile stress that goes to zero when the SFT is crossed and subsequently the coating goes into compression before temperatures near 3000^{o}F are reached. The only way to determine the SFT is to measure the average residual strain in the coating islands at room temperature after the craze cracks have formed, since we do not know at what temperatures the craze cracks form and the amount of stress remaining in the coating islands when they form.

Testing was initiated at Southern Research Institute to experimentally measure the average residual strains in the material system at room temperature and the temperature when cracks close. The

preliminary experimental data yielded crack closure to occur at temperatures between 525 and 1250°F.

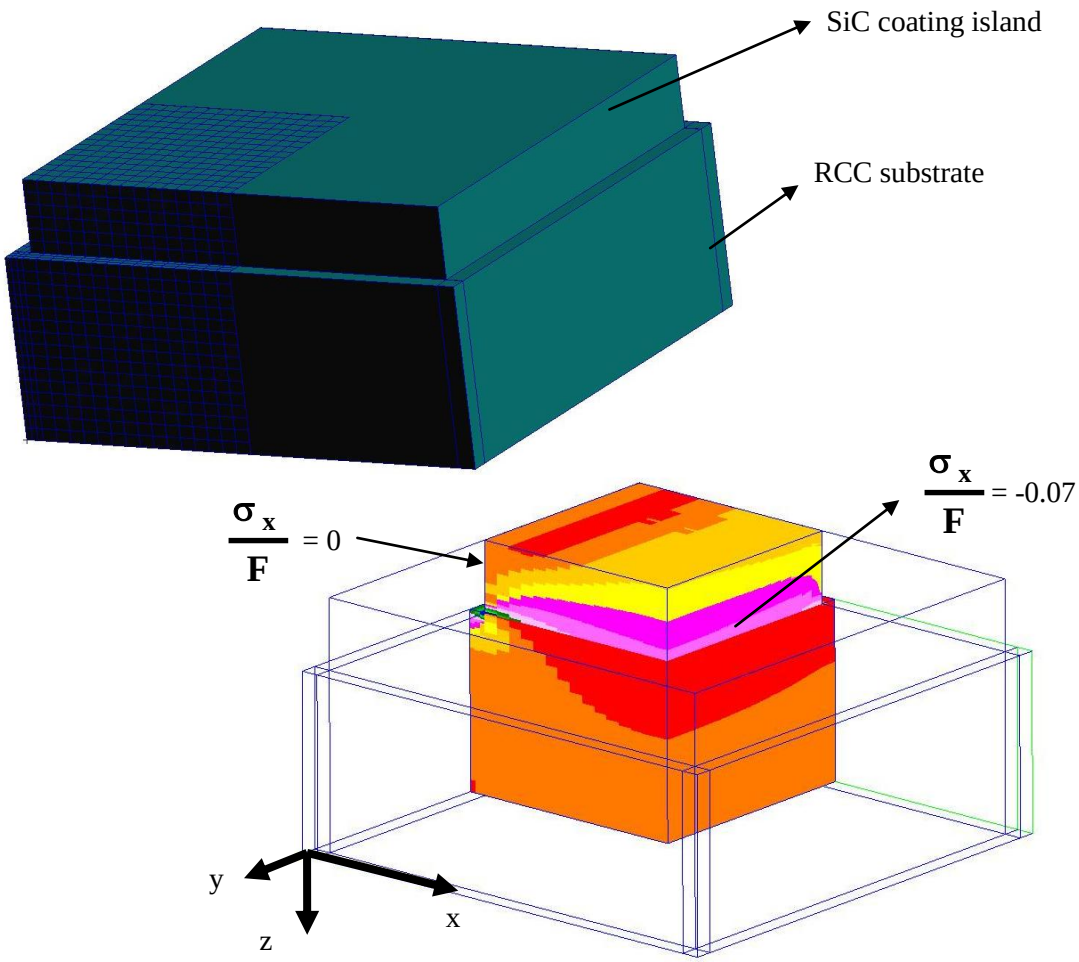

Fig. 7 Three-dimensional analysis model of SiC coating island bonded to RCC substrate along with normal in-plane stress contours for ΔT = 300F.

The SFT was predicted to be approximately 1000°F from measuring residual strain using X-ray diffraction on a flat specimen. Variations in SFT can be attributed to variability in craze crack spacing and coating thickness. Additionally, the curvature in the joggle needs to be considered which could result in the residual strain in the joggle differing from the residual strain measured in the flat test coupons. Consequently, the high sensitivity of stress with variations in SFT (see Fig. 6) that can exist in the RCC leading edge panels must be acknowledged in presenting structural response for the joggle configuration. In general, there can be a large variability in the stress magnitudes experienced by joggles operating at the same temperature due to variation in actual SFT, coating thickness, craze crack spacing, and other possible influences.

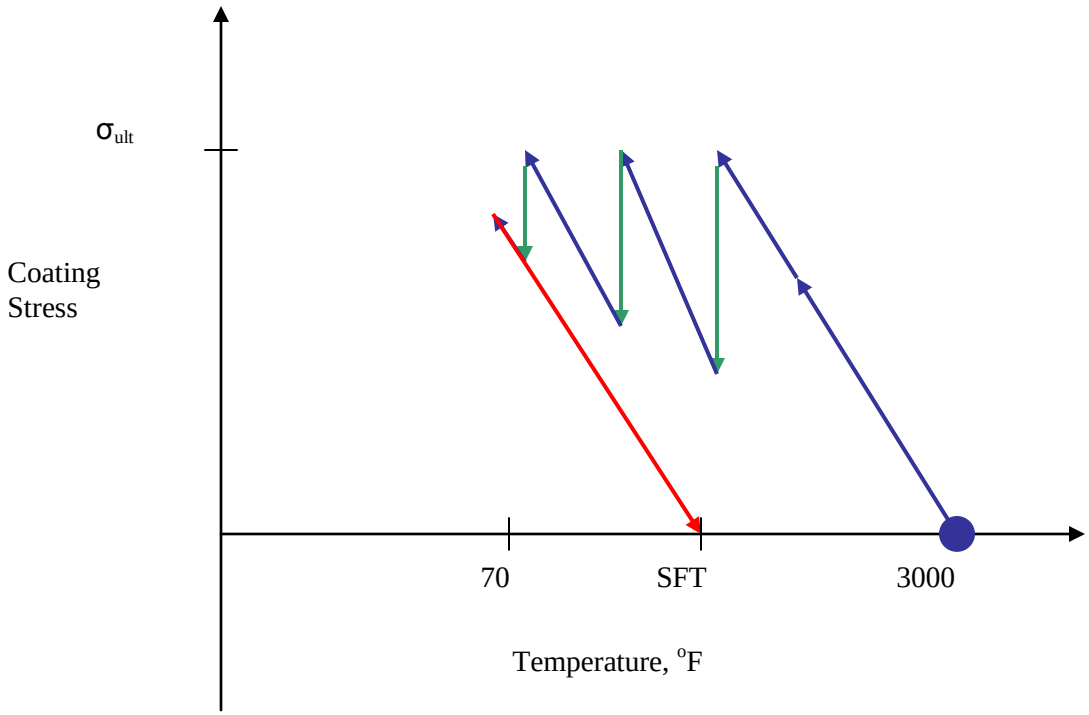

Fig. 8 Hypothesized illustration of SFT in coating.

Preliminary Plane Strain Analyses

A preliminary plane strain analysis model was developed here during the early stages of the investigation to generate a quick look at stresses in the joggle region and determine if stresses during re-entry are a concern for further investigation. Using simplified isotropic properties, a SFT of 700°F and applied temperature of 2900°F, significant stresses were predicted in the joggle region at the coating interface. A separation was introduced into the model at the interface between the coating and RCC substrate to evaluate the effect on the thermostructural response during re-entry. The predicted deformation and maximum principal stress, σ_p, are displayed in Fig. 9. As depicted in Fig. 9, the outer separated region bows away from the substrate and a tensile stress concentration is predicted at the crack tip. This structural response has potential to lead to both plastic deformations and growth of the separated region (Ref. 4). Since the plane strain model has an associated conservative assumption that the separation exists infinitely in the panel chordwise direction, the predicted response could be unrealistic, and thus the need for a detailed three-dimensional model was identified.

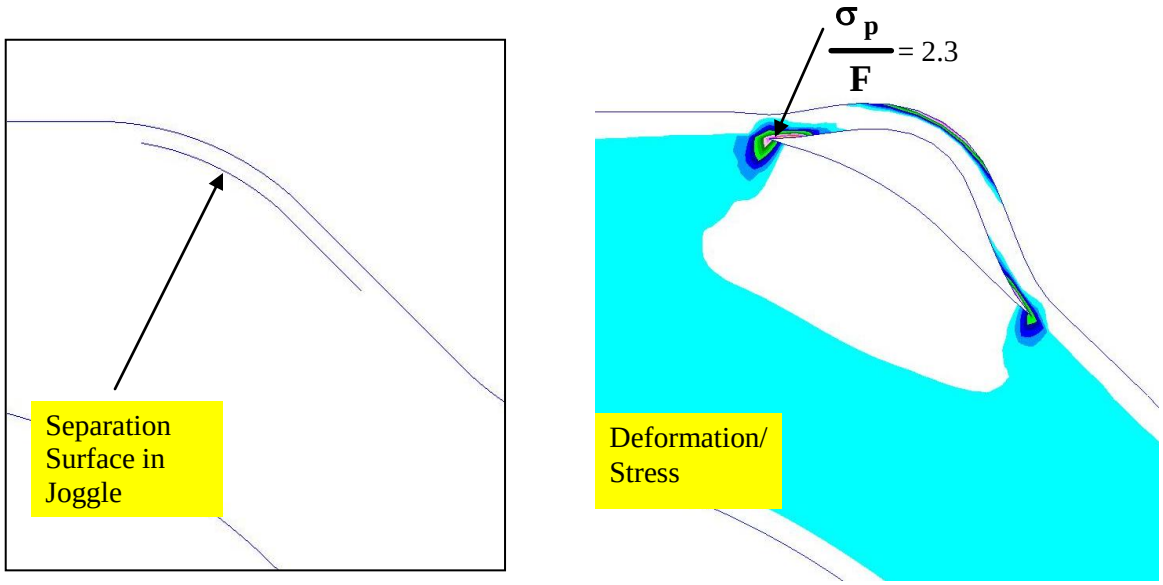

Fig. 9 Plane strain finite element model including separation surface and associated deformation and thermal stress response.

Three-Dimensional Models

The three-dimensional models of the joggle region originated from a solid geometry model of Panel 10 which was imported into PATRAN (Ref. 7). From the full-scale panel model, an 8-inch by 4-inch region adjacent to the panel apex and slip-side panel rib was extracted as shown in Fig. 10, along with the geometry detail through the panel thickness at an apex slice. The acreage area of the panel consists of a thickness of 0.233 inches which is the typical thickness for 19-ply coated RCC. Very locally in the curved region of the joggle the thickness increases to a maximum of 0.28 inches and then decreases back to 0.233 inches aft of the curved region, which is representative of the increase to 22 plies in the joggle. Based on averages from microscopy data, a uniform coating thickness of 0.04 inches is defined throughout the joggle model. Thus only the RCC substrate thickness increases in the joggle region. Although craze cracks are present in the coating at room temperature, these models assume that the cracks are closed at the SFT allowing the coating to be modeled as continuous for the high temperatures experienced during re-entry.

In addition to the 8-inch by 4-inch geometry, further cuts were made from the extracted local joggle geometry to create the 4-inch by 4-inch model without the rib. These two geometries were chosen based on the specimen size capability of the Multi-parameter Mission Simulation Facility (MMSF) at NASA Langley which was being considered for the testing of joggle specimens by thermal cycling using re-entry heating thermal profiles. Although the MMSF could accommodate as large as the 8-inch by 4-inch specimen, the 4-inch by 4-inch specimen was more attractive for the ability to maintain the desired temperature profiles on the specimens. Additional reasons for considering the 8-inch by 4-inch is to have enough material to mechanically restrain the boundaries and apply mechanical load if needed to introduce global loads into the joggle specimen.

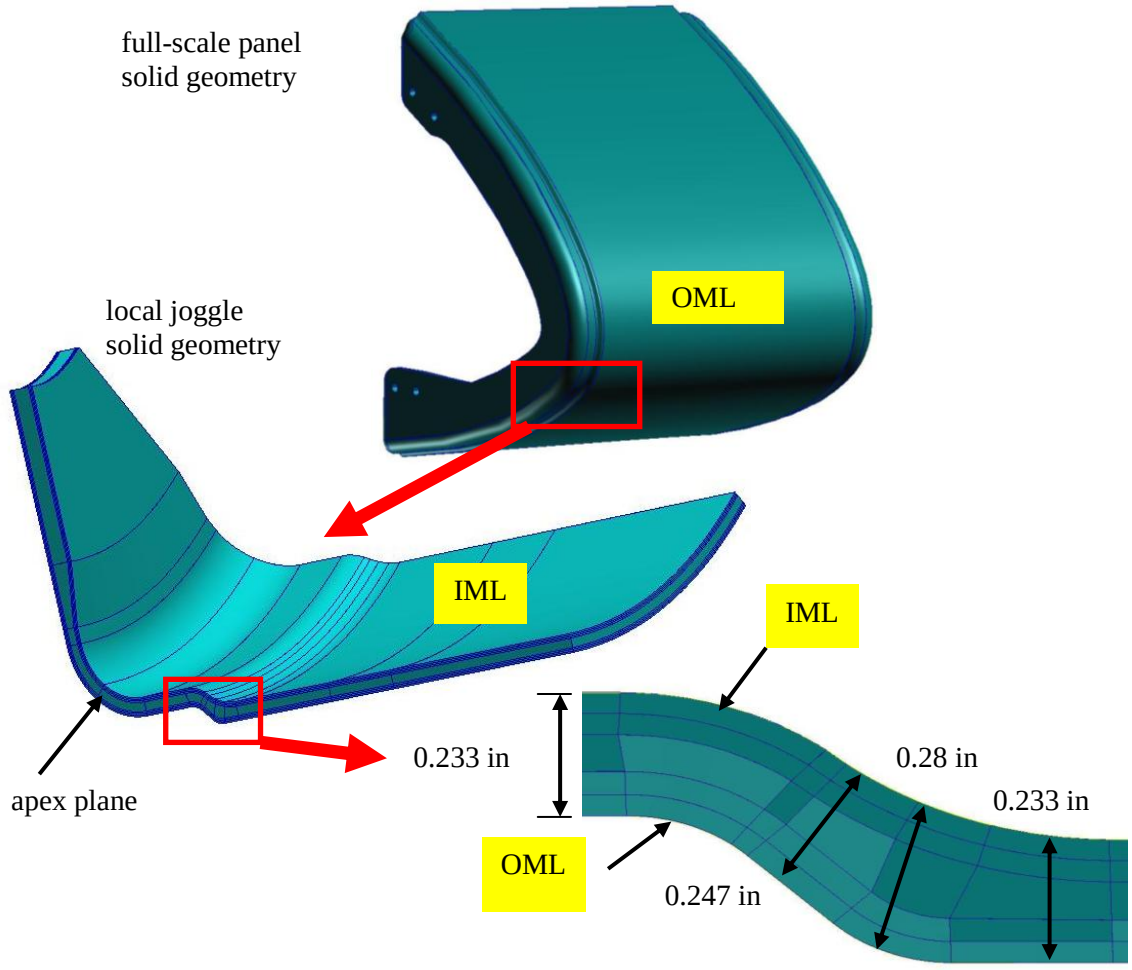

Fig. 10 Full-scale Panel 10 solid geometry along with local 8-inch by 4-inch model geometry and close-up view showing detailed dimensions through the thickness of the panel joggle.

Both finite element models are displayed in Fig. 11 along with the laminate coordinate system utilized for evaluating the results. The laminate coordinate system was based on elements defined consistently to have an element coordinate system with the x-component following the in-plane laminate properties in the panel span direction, the y-component following the in-plane laminate properties in the panel chord direction and the z-component following the laminate properties through the thickness of the panel. The typical element size is 0.04-inches in the x-direction, 0.08-inches in the y-direction, and 0.02-inches in the z-direction for the three elements adjacent to the outer mold line (OML) and inner model line (IML). This meshing yielded two elements representing SiC coating and five elements for the RCC substrate through the thickness of the panel.

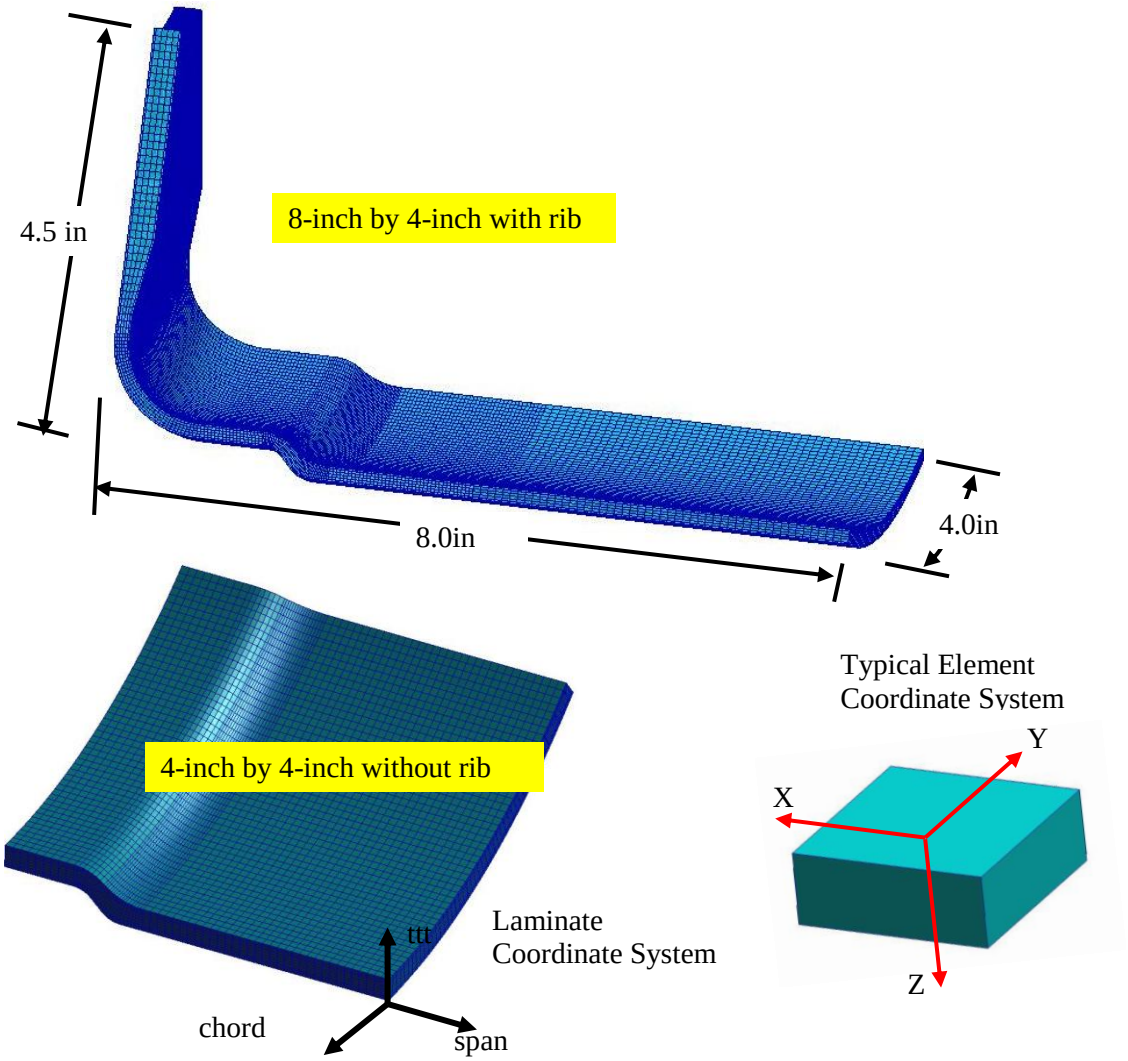

Fig. 11 Finite Element Models (FEM) and associated laminate and element coordinate systems.

Material Properties

Most of the material properties used in the models for both the SiC coating and RCC substrate were generated from testing the materials at Southern Research Institute. Both the coating and substrate material models included temperature-dependent materials properties. Since the shear strength of the SiC was not available, a conservative approach using the RCC interlaminar shear strength for the homogeneous SiC shear strength was adopted since data from testing coated RCC, where the SiC coating and RCC substrate were loaded in equivalent shear, had always resulted in RCC failure for all tests (Ref. 8).

Thermal Loading

Transient thermal analyses had been conducted at Boeing Huntington Beach on a shell model of Panel 10. The predicted peak temperatures that occurred on the panel and joggle region occurred at 800 seconds into re-entry and are displayed in Fig. 12. As shown on the panel OML, a peak temperature of 2680°F occurred at the joggle, where the corresponding predicted IML element temperature was 2480°F (not shown). In consideration of these temperature results, four thermal load cases are created for applying to the local joggle models to parametrically study the sensitivity of the stress solution with respect to the peak operating temperature and spatial temperature gradients. The four load cases include: 1) Uniform Applied Temperature, 2) Insulated IML, 3) Insulated Rib, and 4) Insulated IML and Rib. These cases were named based on what would be needed if an experiment was determined necessary to replicate the thermal gradients, i.e., for load case 2) the IML would need to be insulated to try to achieve the desired thermal gradient through the thickness of a specimen. Nevertheless, steady-state thermal analyses were performed to achieve the temperature distributions using prescribed temperature boundary conditions for the analysis effort, based on the desired global panel temperature results shown in Fig. 12. Prescribed boundary conditions were used to simply generate the desired temperature distributions, as opposed to actually modeling insulation in the finite element model. The reason for analyzing these cases included both to study the effect of spatial thermal gradients on the thermal stress solution and to determine the accuracy of thermal distributions needed to replicate thermals stresses adequately on a laboratory test specimen. Contour plots showing temperature distribution results for the thermal cases on the 4-inch by 8-inch model with rib are displayed in Fig. 13. Where case 1) is the simplest uniform temperature case that can most easily be achieved during testing, case 4) most accurately represents the predicted temperature distribution occurring at the joggle during re-entry. The cases were created to independently investigate the effect of the temperature gradient through the thickness and the temperature gradient across the span on the thermal stress solution of the joggle. The cases also represent thermal distributions that may be achievable during testing by insulating regions of the test specimen.

Three-dimensional Baseline Analysis Results and Discussion

Structural analyses were performed using NASTRAN's nonlinear static analysis capability (Ref. 5). The nonlinearity is due to the temperature dependency of the material properties and otherwise linear elastic material behavior is assumed in the models. Analyses were executed on each of the two local joggle models previously described and for each of the thermal load cases. For both models, boundary constraints were applied only to prevent free body motion and thus the model boundaries were free to expand and/or contract under the thermal loading conditions. Unless otherwise noted, a SFT of 700°F is used in the models.

The baseline case studied is the uniform thermal load case, Case 1, where T=2680°F, applied to the 4-inch by 4-inch joggle model with no rib. In the subsequent figures, stress results in the SiC coating and RCC substrate will be shown individually for clarity in presentation. The values shown are the ratios of the stress values to the corresponding average ultimate strength of the material at the peak joggle temperature which is expressed as SF, the stress factor,

$$SF_i = \frac{\sigma_i}{F_i} \tag{6}$$

where F is the average ultimate strength of the material component at the peak joggle temperature in the i-th material coordinate direction. In the forthcoming figures, values of SF_i much less than one are considered not significant, and the focus is on values of SF_i near or greater than one, where thus the stress may exceed the actual ultimate strength of the material.

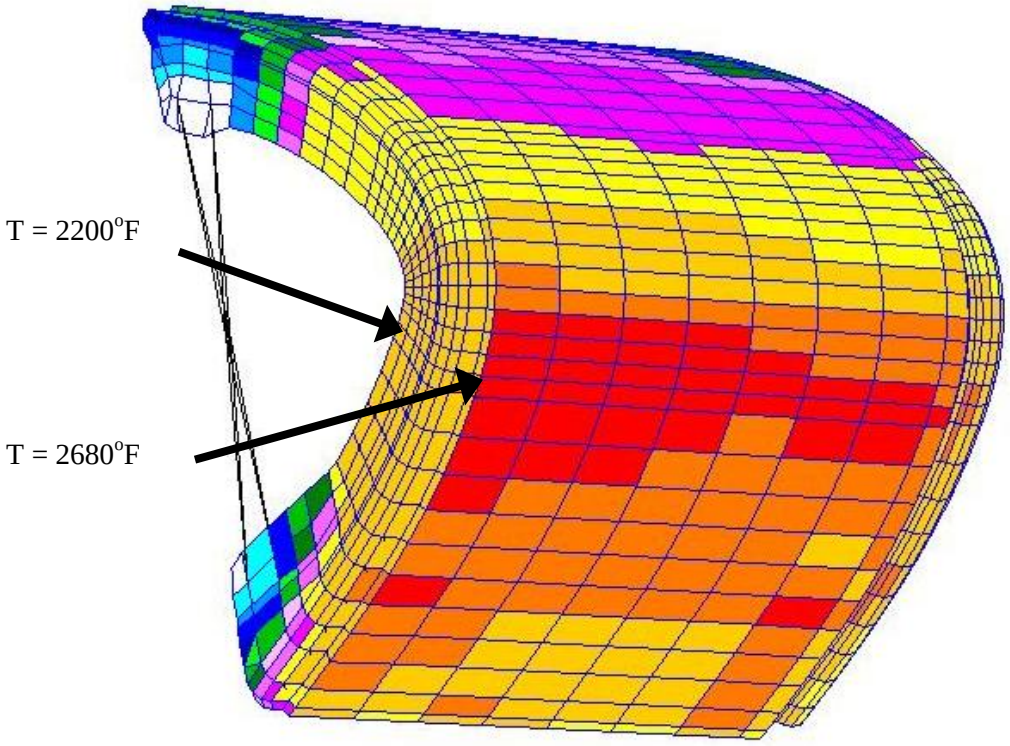

Fig. 12 Peak joggle temperatures predicted on global shell model of Panel 10 at t = 800 sec.

For the homogeneous SiC coating, a peak stress occurred in the spanwise direction in the curved portion of the joggle at the interface between the OML coating and RCC substrate. The span direction stress distribution in the OML coating elements is displayed in Fig. 14. These results indicated that significant compressive stresses arise in the coating due solely to thermal loading. The maximum spanwise stress in the coating is located on the inner surface adjacent to the RCC substrate and is confined to the curved joggle region where the RCC substrate has an increase in thickness from the acreage region. The stress is significant and nearly constant along the entire chord of the joggle except near the free edges where a spike in the span stress component is observed. This free edge effect is a concern for test specimens and will be discussed later in this report.

For the RCC substrate, the spanwise stress distribution is displayed in Fig. 15. Unlike the coating stress distribution where a peak stress was observed on the joggle, the peak spanwise stress in the RCC substrate occurs further down where the curvature changes direction, which would be located under the T-seal. Alternatively, at the curved joggle region a slight decrease in the span stress is observed in the RCC

substrate. What is of utmost significance in the RCC substrate is the through the thickness stress predicted and displayed in Fig. 16. Revealed is a tensile interlaminar normal stress concentration that exists only in the curved portion of the joggle at the interface with the OML coating. This stress component is the most severe component predicted in the analysis and exceeds the average interlaminar tensile (ILT) strength of the RCC substrate. Similar to the coating stress, the stress is nearly constant along the chord of the joggle except near the free edge where a local increase occurs. To observe better the stress distribution through the thickness near the center of the finite element model, a section of elements was taken at the center and the local results are displayed in Fig. 17. In the through the thickness direction at the joggle, in approaching the RCC surface adjacent to the OML coating, the stress increases from relatively benign values to values in excess of the ILT strength at the outermost element adjacent to the SiC coating. Clearly, a through the thickness stress concentration exists in the RCC substrate which is localized in the curved portion of the joggle at the interface with OML SiC coating.

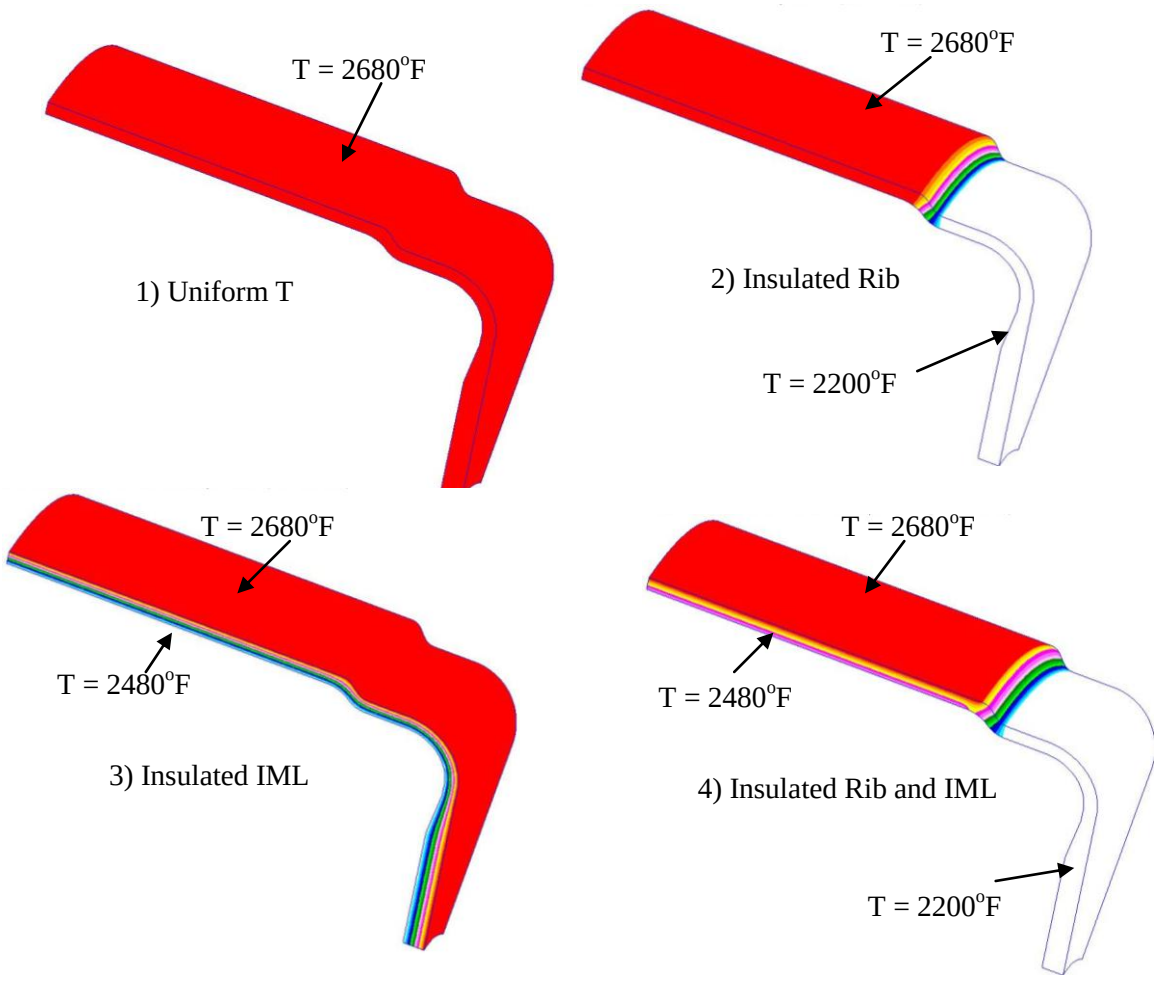

Fig. 13 Temperature distribution contour plots for thermal load cases.

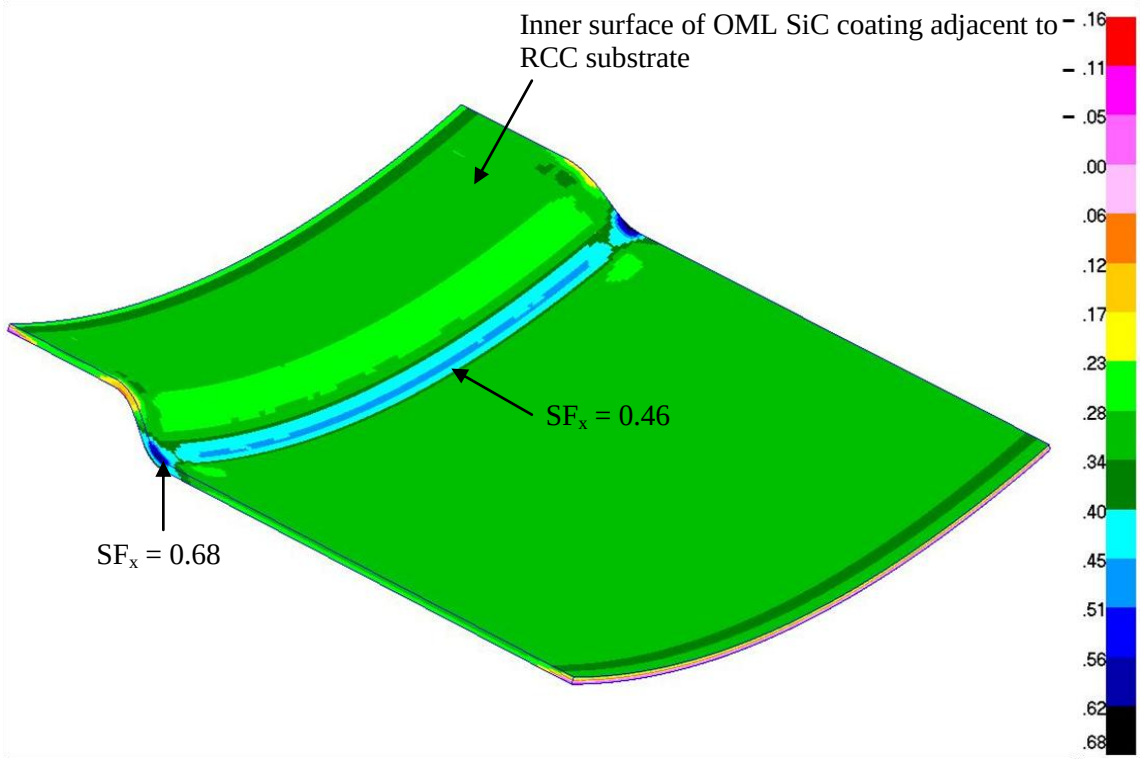

Fig. 14 Compressive stress distribution in spanwise direction in OML SiC coating for baseline analysis.

A convergence study was performed on the results using a refined mesh model. The model was refined to include twice as many elements in each material coordinate direction in the joggle region. Results of this study showed negligible change in the in-plane stress prediction values. For the peak through the thickness ILT stress predicted, a 6% increase in the element adjacent to the OML SiC coating interface was predicted. The ILT stress then decreased while remaining significant within the next two elements away from the interface. Consequently, the peak magnitude of the ILT stress predicted at this location can only be considered approximate, although the presence of a critical stress concentration is clear.

In general, significant magnitudes of stress exist in the joggle region on the panels when high temperatures are experienced from the high heat fluxes occurring during re-entry. The predicted stresses in the joggle region are more severe than panel stresses away from the joggle. The severe through the thickness stress concentration is due to a highly localized phenomenon associated with the combined effect of high curvature in the joggle in conjunction with the high temperatures experienced in the material system composed of two materials with differing thermal expansion coefficients. This phenomenon can only be captured with the materials modeled discretely with respect to their material properties and with a model containing sufficient elements through the thickness to depict the stress concentration. Unfortunately, the global shell analysis model was not able to capture this critical stress component inherent in the design of the joggle. Importantly, one should be aware that in a flat plate with the coating modeled discretely from the substrate, the through the thickness stresses are zero when subject to a thermal load only. Thus the phenomenon of a through the thickness stress concentration requires the presence of a finite radius of curvature as is the case with the joggle designed with a quarter inch radius of curvature.

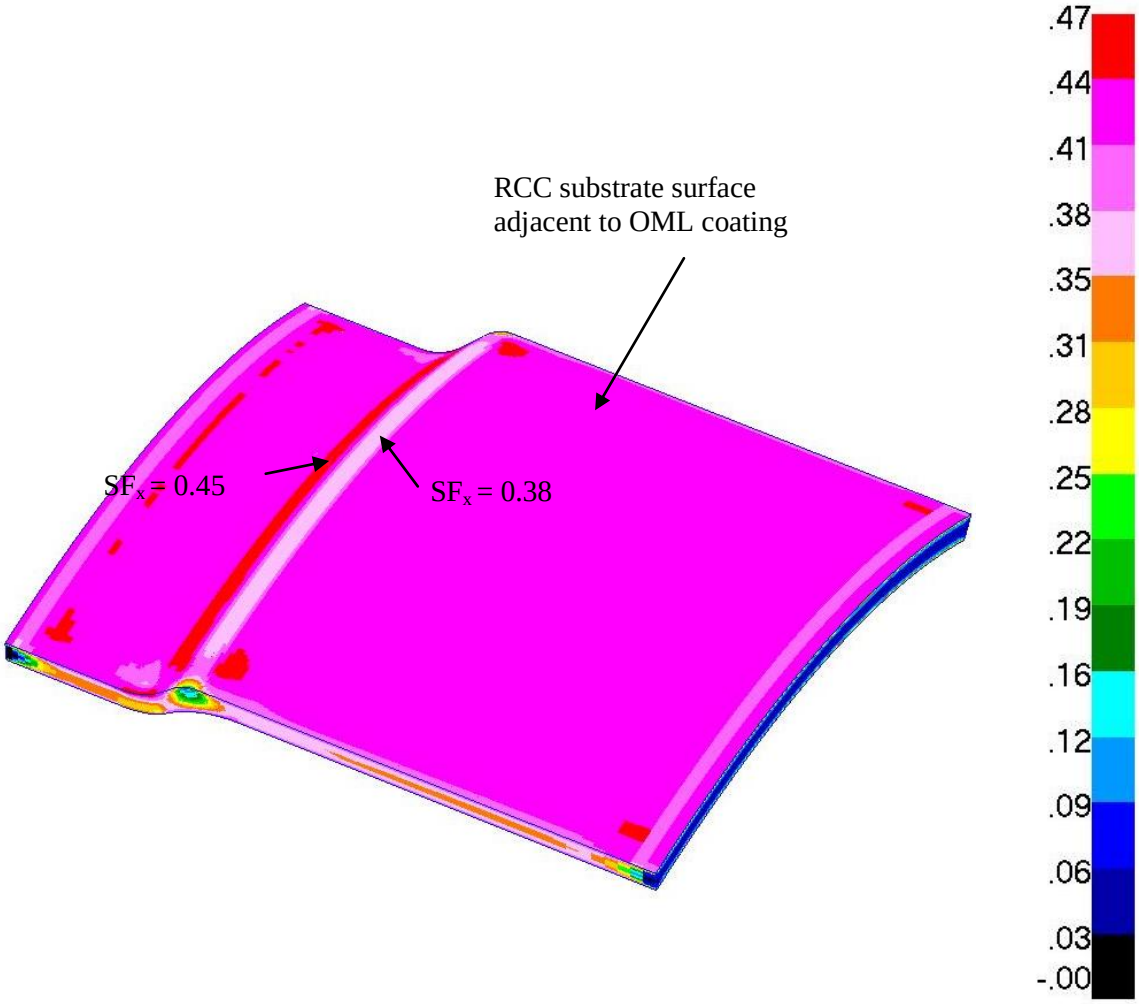

Fig. 15 Stress distribution in spanwise direction in RCC substrate for baseline analysis.

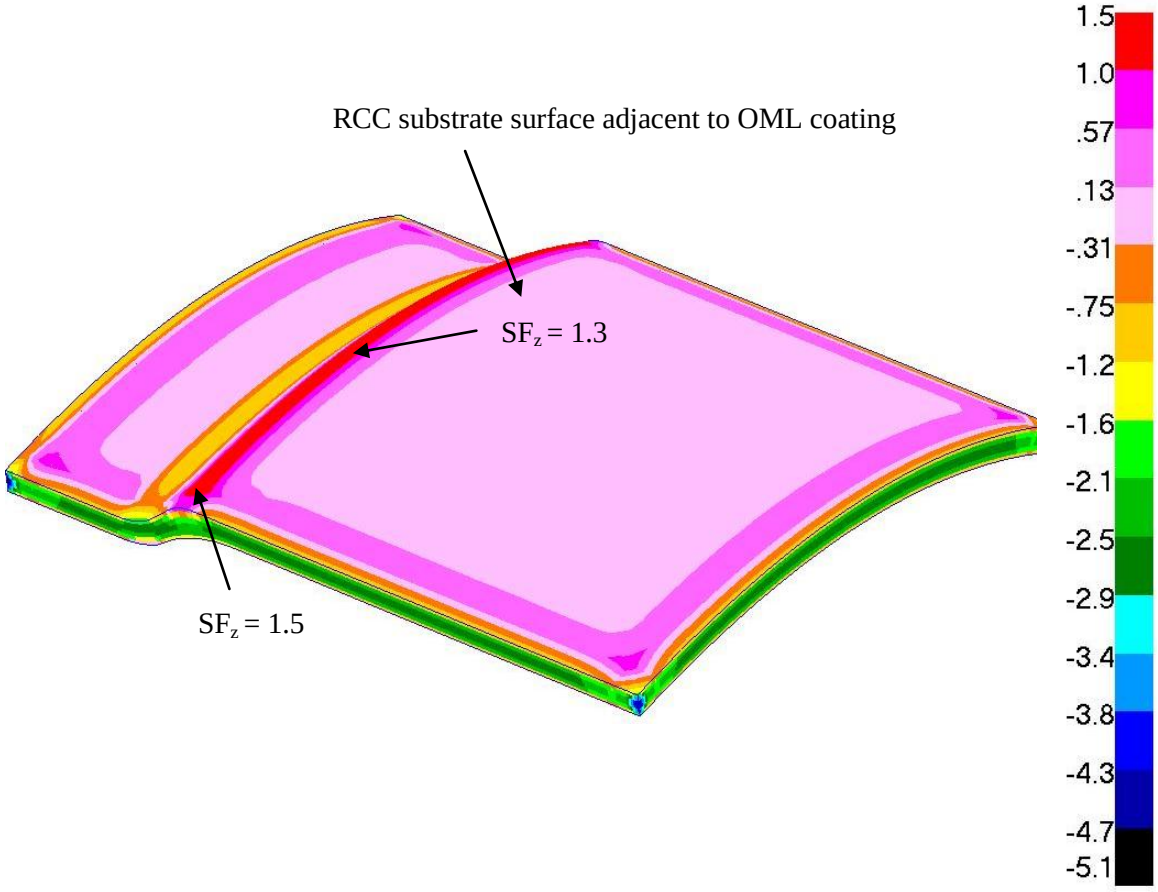

Fig. 16 Stress distribution through the thickness in RCC substrate for baseline analysis.

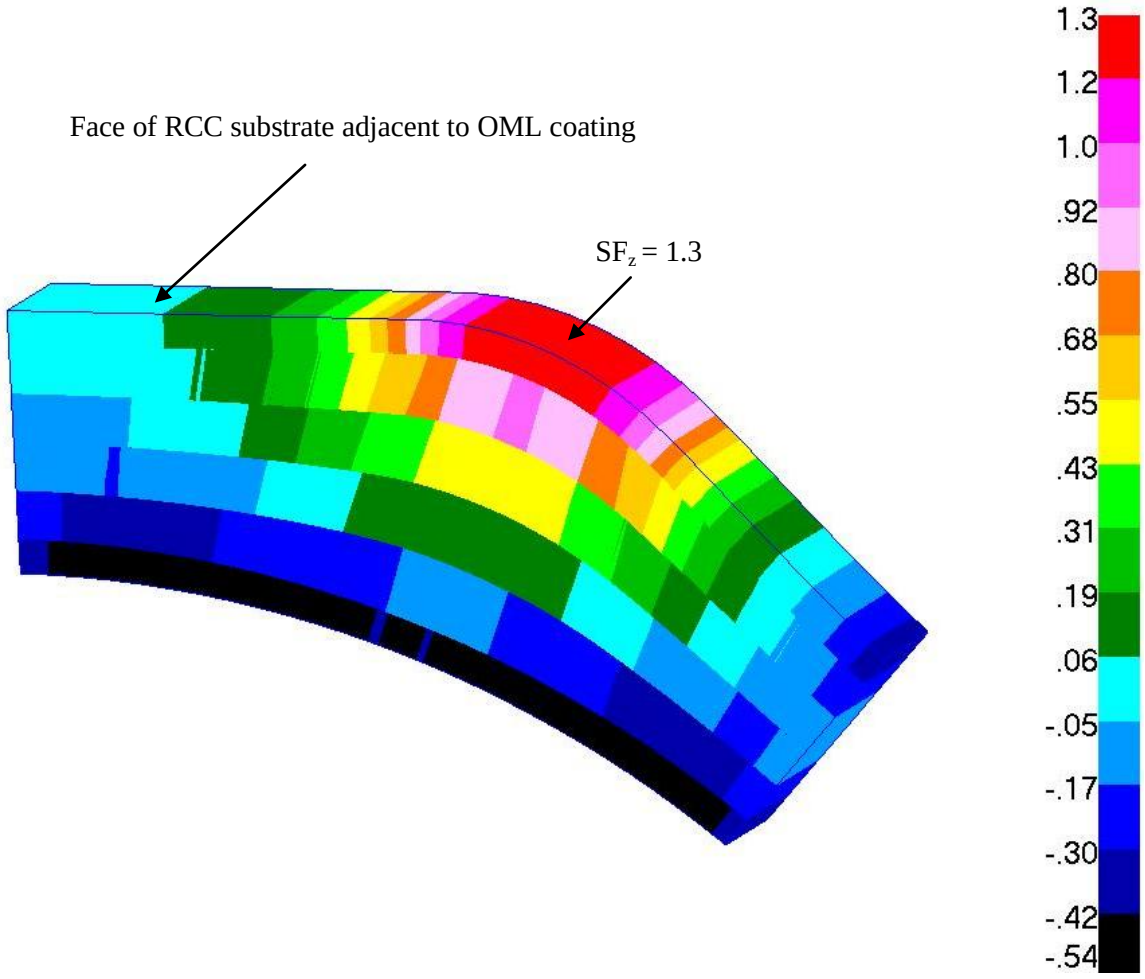

Fig. 17 Stress distribution through the thickness in RCC substrate elements taken from center of finite element model in baseline analysis.

Parametric Study: Thermal and Geometric Sensitivity

The main objective of the parametric study is to define an optimal test to best replicate the state of stress occurring in the panel joggle region during re-entry. Testing can then be performed on local joggle specimens to determine experimentally if the loading condition experienced during re-entry leads to the observed material separations and spallation events. Both test specimen size and the loading conditions were considered in this analytical evaluation. A secondary objective of the parametric study is to evaluate the detailed state of stress occurring in the joggle during re-entry and its sensitivity to potential variations that could exist in the local thermal loading condition.

Analysis of joggle geometries included the 8-inch by 4-inch model with the rib and the 4-inch by 4-inch model without the rib as shown in Fig. 11. Each model is subject to the four thermal loading

conditions shown in Fig. 13. All peak stress factors occurring in the center joggle region, away from free edges, are displayed in Table 1. The peak values are displayed for each stress factor component in the RCC substrate and in the SiC Coating. For each case shown, the peak stress factor remained in the same location despite the variation in geometry or thermal load condition. The interlaminar normal stress distribution for the 8-inch by 4-inch model, when subject to the insulated rib and IML load condition, is shown in Fig. 18. A close-up of the stress distribution through the thickness of the RCC in the joggle center section is shown in Fig. 19. Comparing these stress factors to the corresponding stress factors predicted in the 4-inch by 4-inch model subject to the uniform thermal load (shown in Figures 16 and 17) clearly indicates that changing the extent of the geometry modeled or the thermal spatial gradients in the joggle region did not affect the location of the peak stress component or the general character of the distribution of the stress component in the joggle.

Table 1. Peak stress factors occurring in the center joggle region

	8-inch by 4-inch with rib				4-inch by 4-inch without rib			
	Tuniform	Ins. Rib	Ins. IML	Ins. R & I	Tuniform	Ins. Rib	Ins. IML	Ins. R & I
RCC SFx	0.45	0.46	0.45	0.45	0.46	0.46	0.45	0.45
RCC SFy	0.44	0.39	0.43	0.40	0.43	0.41	0.44	0.41
RCC SFz	1.30	1.18	1.42	1.26	1.28	1.16	1.38	1.24
RCC SFxy	0.00	0.01	0.01	0.01	0.00	0.01	0.01	0.00
RCC SFyz	0.01	0.01	0.01	0.01	0.00	0.01	0.01	0.01
RCC SFzx	-0.11	-0.16	0.20	0.15	-0.10	-0.18	0.17	-0.12
SiC SFx	-0.46	-0.42	-0.49	-0.44	-0.46	-0.42	-0.48	-0.44
SiC SFy	-0.33	-0.42	-0.42	-0.45	-0.34	-0.39	-0.40	-0.40
SiC SFz	0.07	0.06	0.08	0.06	0.06	0.06	0.07	0.06
SiC[a] SFxy	-0.08	0.15	-0.16	0.10	0.01	0.09	0.14	0.03
SiC[a] SFyz	-0.01	-0.01	-0.02	-0.01	-0.01	-0.01	-0.01	-0.01
SiC[a] SFzx	0.37	0.30	0.44	0.37	0.37	0.31	0.43	0.37

a Interlaminar shear strength for coated RCC used for SiC strength which would be greater.

Of most interest here is the difference of the stress between the 8-inch by 4-inch model with the insulated rib and IML, where the loading condition best replicates the re-entry thermal load, and the 4-inch by 4-inch model with the uniform temperature distribution, which would be the simplest test that could be most efficiently accommodated experimentally. Only minor changes in the actual peak values for these cases are observed. The largest difference is observed with the chordwise y-direction stresses in the coating between the cases. As expected this stress component is largest when thermal x-direction spatial gradients are largest, where the cooler rib temperatures constrain thermal expansion leading to large compressive stresses at the joggle. However, this y-direction stress component is much less critical

than the through the thickness ILT stress component occurring in the RCC substrate. This ILT stress component and the other significant stress component in the coating, the interlaminar shear stress, show negligible differences.

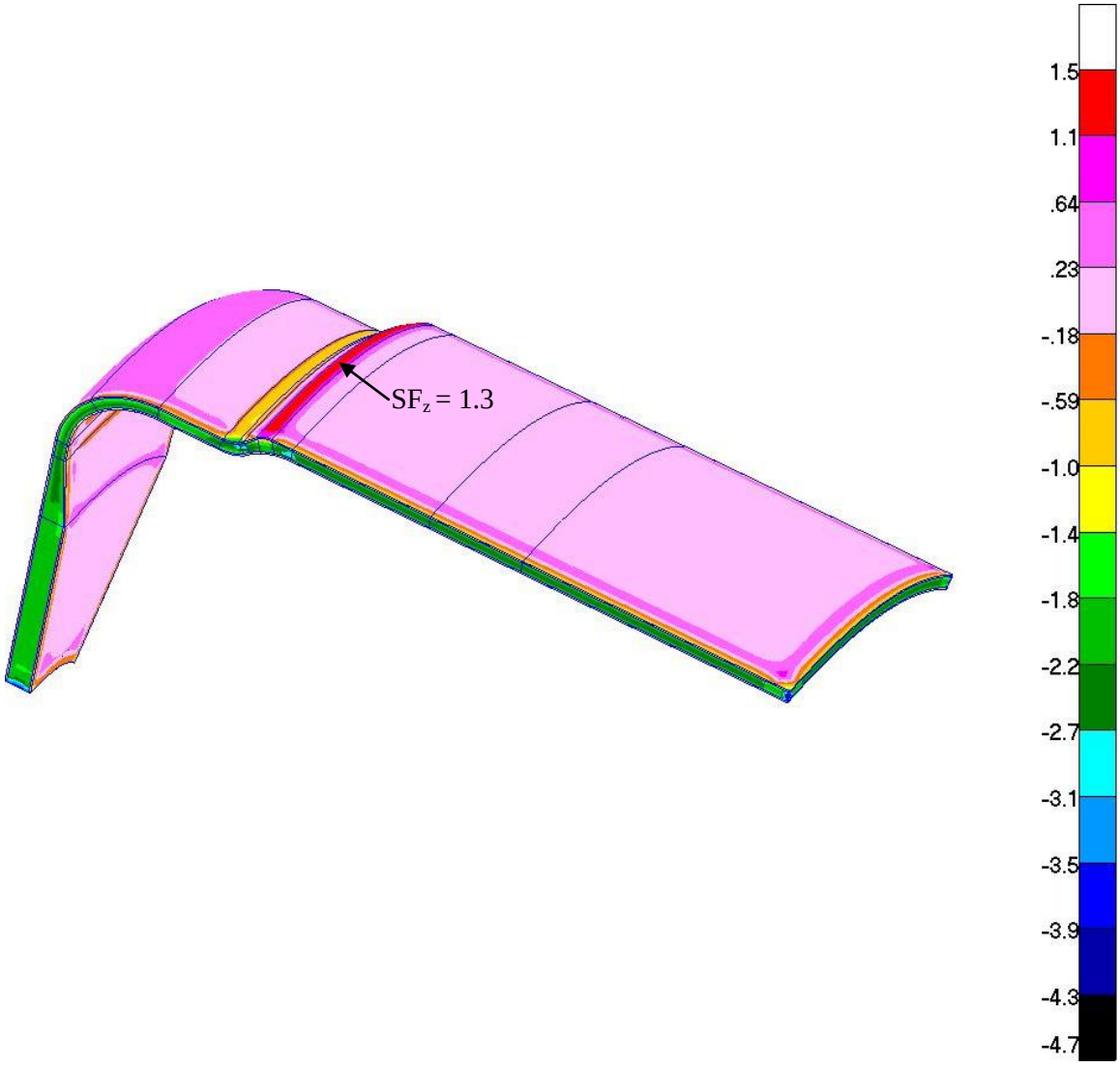

Fig. 18 Stress distribution through the thickness in RCC substrate elements from 8-inch by 4-inch model subject to thermal load case 4, insulated rib and IML.

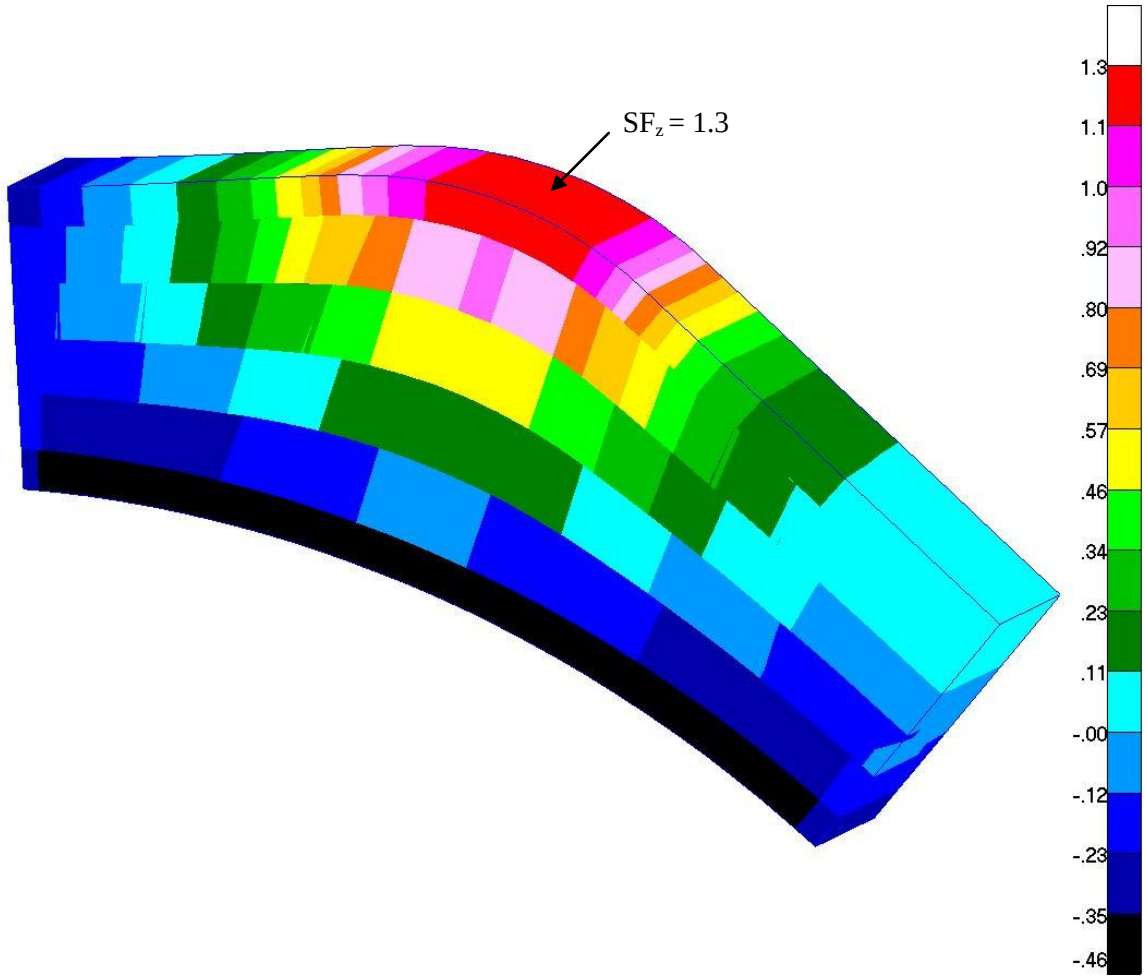

Fig. 19 Stress distribution through the thickness in RCC substrate elements taken from center of finite element model for 8-inch by 4-inch model subject to thermal load case 4, insulated rib and IML.

The sensitivity of the joggle stress state to changes in the value of the applied temperature and the assumed SFT is also studied. Using the uniform temperature thermal load case on the 4-inch by 4-inch specimen, a uniform temperature of T= 1700, 2100, 2400, 2680(baseline case), and 2900^{o}F was applied. The critical ILT stress factor results are presented in Fig. 20. The peak ILT stress factors are plotted as a function of the uniform applied temperature. Each curve is for an assumed value of the SFT. In each case the stress decreases appreciably with decreasing applied temperature as expected due to the decrease in the thermal loading condition. Clearly the ILT stress becomes less critical at lower applied temperature and at higher assumed SFT, due to the associated decrease in the thermal load (see Eq. 2). Not shown, the peak in-plane stresses predicted also decrease similarly with decreasing applied temperature.

Care must be taken during validation testing to prevent peak stresses occurring at panel free edges. The analysis indicates that the free edges experience spikes in stress compared to the center joggle region away from the boundaries. However, panel free edges are not exposed to the high temperatures associated

with the stress spikes. There are no free edges in the vicinity of the panel joggle where the highest temperatures occur. If a failure during a test initiated at a hot free edge the failure would not be representative of a failure that would occur during re-entry. Consequently, keeping the free edges cooler on a test specimen should be considered to lower free edge stresses, leaving the peak stresses to occur in the interior region of the specimen.

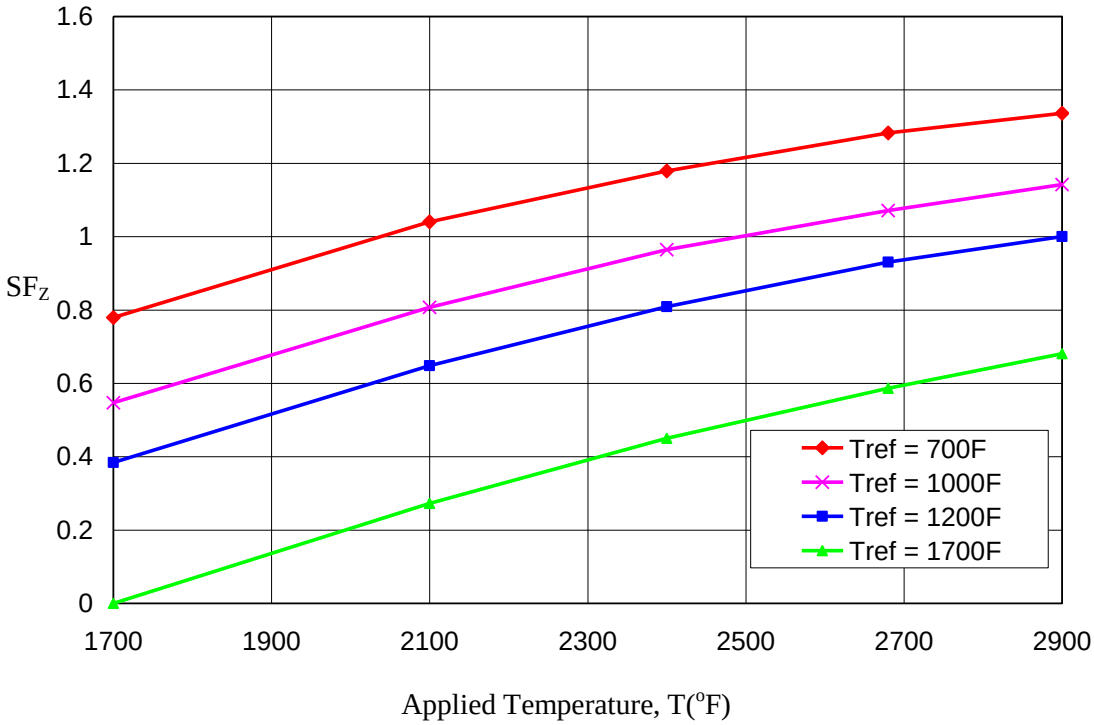

Fig. 20 Peak predicted ILT stress factor for varying applied temperature and assumed SFT values.

Overall, evaluation of the results indicates that the state-of-stress at the joggle is relatively insensitive to potential variations in spatial gradients of the temperature that could be present in the vicinity of the joggle during re-entry. Alternatively, the actual peak temperature occurring at the joggle dominates the response in influencing the magnitude of the critical stress experienced at the joggle. Based on results of the parametric study, the highest stresses in the joggle are predicted to occur at the time during re-entry when the highest temperature is experienced at the joggle location.

Significant stress magnitudes are predicted in the local joggle analysis effort compared to the stress magnitudes that had been predicted in the joggle region with the global shell model. The contribution to the total local stresses from the global loads is evidently negligible. Thus, a detailed global panel analysis model is not necessary to predict the local joggle state of stress nor is mechanically restraining the edges of a test specimen or applying additional mechanical input loads needed to replicate global panel load conditions on the boundaries of the local model. Additionally, with the insensitivity of the local results to

the modeling of differing local model sizes, the baseline 4-inch by 4-inch local geometry model with a uniform thermal load and without external mechanically applied loads is sufficient to adequately replicate local stresses in the joggle that occur during re-entry. Therefore, a 4-inch by 4-inch test specimen thermally cycled to the peak operating temperature is concluded to be an adequate test for generating the critical state-of-stress experienced in the joggle during re-entry.

Failure Analysis

Heretofore analysis of the local joggle model has provided insight into the state-of-stress occurring locally in the joggle as part of the full scale panel for the hottest temperatures incurred during re-entry. Since the most severe stress in the joggle is predicted to occur when the temperatures are highest during re-entry, this state of stress is considered for failure analysis.

The coated RCC material system falls into the category of a Ceramic Matrix Composite (CMC). Typically, the Maximum Stress/ Strain Failure Theory is considered an applicable failure theory for CMC materials due to the brittle nature of the material system, where Mohr's hypothesis for brittle material states that fracture occurs in the plane where normal and shear stresses exceed the strength of the fracture plane. Previous work in the area of failure criteria for CMC materials has even defined Maximum Stress/Strain Failure Theory as the best failure theory for CMC materials (Ref. 9). The maximum stress failure criterion predicts fracture to occur for $\sigma_i > F_{ui}$ on the plane normal to the direction of the maximum stress. Here, F_{ui} is the specific ultimate strength in one of the principle material directions of the composite material system. In referring to Fig. 20, which plots SF_z using the average ultimate strength in the through the thickness direction, F_{uz}, failure would be predicted, on average, for $SF_z > 1$. Due to inherent variations in specific aspects of the joggle, which could affect the stress and variations in ILT strength, the exact temperature a specific joggle will fail at is ambiguous. Also, the ILT strength material property was generated on flat coupon specimens, where the actual value for curved joggles could be different due to manufacturing variations (e.g., compaction, porosity, etc.).

Alternative to the maximum stress failure criterion, which is conservative when nonlinear material behavior occurs, the maximum strain failure criterion is also considered here. Maximum Strain Failure Theory predicts failure to occur when the peak predicted strain exceeds the ultimate strain in a material coordinate direction, or for a strain factor, $StF_i > 1$ where

$$StF_i = \frac{\varepsilon_i}{\varepsilon_{ui}} \tag{7}$$

and ε_{ui} is the ultimate strain in the i-th material direction. For the baseline case, the maximum strain failure theory predicts a strain factor of $StF_z = 0.67$ using the average ultimate strain. Although this is lower than 1 for the average strain value used here, lower bound strain data exists for ultimate strain values at approximately 50% of the average value used here (Ref. 10). In this reference, twelve specimens were tested and the average value was at 75% of the average value being used here. Using the lower bound strain value would result in a strain factor of 1.3, where failure is predicted. Consequently for the baseline case the predicted strain value exceeds the lower bound strain data and thus the potential

for failure exists. Considering a 50% lower bound on the ultimate strength value (Ref. 11) and referring to Fig. 20, for a SFT of 1000°F, the potential for failure to occur is observed to exist at temperatures as low as approximately 1700°F.

Overall qualitative observations can be made in considering the trends displayed in Fig. 20. Clearly, the potential for failure increases as the operating temperature of the joggle increases above a threshold temperature that is dependent on the SFT. For joggles with high specific SFT, the probability for failure would be less than for joggles with low specific SFT. Applying the Maximum Stress/Strain Failure Theory, failure is predicted to occur in the form of a subsurface fracture on the plane normal to the through the thickness direction in the curved portion of the joggle in the RCC at the OML SiC coating interface.

Experimental Validation

Arc-jet testing of local joggle with T-seal specimens was performed in parallel to the current analysis effort under the root cause investigation. Although the objective of the arc-jet testing was to determine if there was local heating augmentation on the joggle due to the step and gap condition with the adjacent T-seal, one of the specimens tested resulted in a joggle subsurface material separation post-test where there was no initial NDE indication prior to the arc-jet test (Ref. 12). This response was of interest here and further study was subsequently initiated to evaluate the infrared imaging data to determine when in the test thermal cycle the material separation first occurred. This investigation identified that the material separation appeared to occur during the ramp up to the peak heating condition, where specimen temperature went from 2500 to 2800°F (Ref. 13). This finding provided experimental data consistent with the current analysis effort in identifying the ramp to peak heating as being the time in the re-entry thermal cycle when a material separation occurred.

Conclusions

Detailed finite element analysis models of the local joggle region were created and utilized to predict the thermostructural response of the joggle during re-entry of the Shuttle Orbiter. Parametric and sensitivity studies revealed the most significant stresses occur in the joggle during peak heating due to the locally high temperature and discontinuity in material properties between the coating and substrate material. At the highest temperatures experienced in the joggle, a critical state of stress is predicted where excess ILT stress occurs in the curved portion of the joggle in the RCC at the interface with the OML SiC coating. The location of this critical stress component coincides exactly with the location of material separations observed with microscopy. Consequently, failure due to excessive interlaminar normal stress occurring at the curved joggle region in the RCC substrate adjacent to the OML SiC coating is concluded to be the cause for the observed material separations. The material separations are predicted to occur during heat up and are most likely to occur sometime between reaching 1700°F and the peak operating temperature for the joggle, where potential for failure increases with increasing temperature. Once a subsurface material separation is present, local geometric changes due to the separation would lead to further variation and uncertainty in the SFT in the separated region and thus, further uncertainty in post material separation analyses. Consequently, thermal cyclic testing is recommended to study the propagation of the failure and to determine the specific flight loading conditions associated with actual spallation of the SiC coating.

Acknowledgements

The authors would like to express their gratitude to the NESC for funding this work and to the individuals:

- Clint H. Cragg, NASA LaRC for supporting this study
- Stephen J. Scotti, NASA LaRC for technical consultations and review
- David N. Brewer, NASA LaRC for his technical review
- Kamran Daryabeigi, NASA LaRC, for providing invaluable experimental validation and technical review
- John Koeing, Southern Research Institute, for measuring the stress free temperature
- Elizabeth Opila, UVA, for her microscopic images of the joggle material separation
- Dave Okimo and Fred Gahyasi, Boeing Huntington Beach, for their NASTRAN global shell model of the leading edge Panels

References

[1] Smith, T.W., "Leading Edge Structural Subsystem Mechanical Design Allowables for Material with Improved Coating System", LORAL Vought Systems, Rpt. No. 221RP00614 Rev. A, October 12, 1994.

[2] Gordon, M. P., Leading Edge Structural Subsystem and Reinforced Carbon-Carbon Reference Manual, Contract NAS9-200000, KLO-98-008, Boeing, October 19, 1998.

[3] MSC NASTRAN Quick Reference Guide, MSC Software Corporation, Santa Ana, CA, 2005.

[4] Walker, S. P., and Warren, J. E., "Thermostructural Analysis of Joggle Region on the Shuttle Orbiter's Reinforced Carbon-Carbon Wing Leading Edge", JANNAF Air-breathing Propulsion Subcommittee Technical Session on Materials and Structures for Airframe and Propulsion Systems, Cocoa Beach, FL, January 26-29, 2009.

[5] Manning, A. S. and Fuchs, S., "Finite Element Analysis of Thermal Stresses in High-power Substrates for Hybrid Circuits", Materials & Design, Vol. 18, No. 2, pp. 61-72, 1997.

[6] NESC Technical Report, "Orbiter Wing Leading Edge Structural Subsystem (LESS) Reinforced Carbon-carbon (RCC) Panel Subsurface Anomaly, NASA Engineering and Safety Center, Req # 07-028-I, August 2007.

[7] MSC Patran, MSC Software Corporation, Santa Ana, CA, 2006..

[8] Williams, A. R., and Koeing, J. A., "RCC Panel 8L Data Report, SRI-ENG-04-04-10359.14", Sourthern Research Institute, Birmingham, Alabama.

[9] Kaiser, C., et. al, “Failure Criteria for FRP and CMC: Theory, Experiments and Guidelines”, Presented at the European Conference on Spacecraft Structures, Materials & Mechanical Testing, 10-12 May 2005, Noordwijk, The Netherlands.

[10] Vaughn, W. L. and Leggette, R. C., “Through Thickness Tensile Modulus of Reinforced Carbon-Carbon”, Test #14 Quick Look Report, Ver. 2, NASA Langley Research Center, May 29, 2007.

[11] “Selected Mechanical Properties of the Space Shuttle Leading Edge Reinforced Carbon-Carbon Material”, SoRI-EAS-76-232, Southern Research Institute, June 1976.

[12] Lewis, R. K. and Rodriguez, A. C., “Panel 10L and 6L Slip Side Joggle Arc Jet Tests", NASA Thermal Design Branch Report, March 2009.

[13] Daraybeigi, K., and Walker S. P., “Detection of Sub-surface Material Separation in Shuttle Orbiter Slip-Side Joggle Region of the Wing Leading Edge Using Infrared Imaging Data From Arc Jet Tests”, JANNAF Air-breathing Propulsion Subcommittee Technical Session on Materials and Structures for Airframe and Propulsion Systems, Cocoa Beach, FL, January 26-29, 2009.

REPORT DOCUMENTATION PAGE

Form Approved
OMB No. 0704-0188

1. REPORT DATE *(DD-MM-YYYY)*	2. REPORT TYPE	3. DATES COVERED *(From - To)*
01- 05 - 2012	Technical Memorandum	

4. TITLE AND SUBTITLE

Thermostructural Evaluation of Joggle Region on the Shuttle Orbiter's Wing Leading Edge

5a. CONTRACT NUMBER

5b. GRANT NUMBER

5c. PROGRAM ELEMENT NUMBER

6. AUTHOR(S)

Walker, Sandra P.; Warren, Jerry E.

5d. PROJECT NUMBER

5e. TASK NUMBER

5f. WORK UNIT NUMBER

869021.05.07.04.11

7. PERFORMING ORGANIZATION NAME(S) AND ADDRESS(ES)

NASA Langley Research Center
Hampton, VA 23681-2199

8. PERFORMING ORGANIZATION REPORT NUMBER

L-20137

9. SPONSORING/MONITORING AGENCY NAME(S) AND ADDRESS(ES)

National Aeronautics and Space Administration
Washington, DC 20546-0001

10. SPONSOR/MONITOR'S ACRONYM(S)

NASA

11. SPONSOR/MONITOR'S REPORT NUMBER(S)

NASA/TM-2012-217571

12. DISTRIBUTION/AVAILABILITY STATEMENT

Unclassified - Unlimited
Subject Category 39
Availability: NASA CASI (443) 757-5802

13. SUPPLEMENTARY NOTES

14. ABSTRACT

An investigation was initiated to determine the cause of coating spallation occurring on the Shuttle Orbiter's wing leading edge panels in the slip-side joggle region. The coating spallation events were observed, post flight, on differing panels on different missions. As part of the investigation, the high re-entry heating occurring on the joggles was considered here as a possible cause. Thus, a thermostructural evaluation was conducted to determine the detailed state-of-stress in the joggle region during re-entry and the feasibility of a laboratory test on a local joggle specimen to replicate this state-of-stress. A detailed, three-dimensional, finite element model of a panel slip-side joggle region was developed. Parametric and sensitivity studies revealed significant stresses occur in the joggle during peak heating. A critical interlaminar normal stress concentration was predicted in the substrate at the coating interface and was confined to the curved joggle region. Specifically, the high interlaminar normal stress is identified to be the cause for the occurrence of failure in the form of local subsurface material separation occurring in the slip-side joggle. The predicted critical stresses are coincident with material separations that had been observed with microscopy in joggle specimens obtained from flight panels.

15. SUBJECT TERMS

Composites; Stress-free temperature; Thermal stress; Thermal structures

16. SECURITY CLASSIFICATION OF:			17. LIMITATION OF ABSTRACT	18. NUMBER OF PAGES	19a. NAME OF RESPONSIBLE PERSON
a. REPORT	b. ABSTRACT	c. THIS PAGE			STI Help Desk (email: help@sti.nasa.gov)
					19b. TELEPHONE NUMBER *(Include area code)*
U	U	U	UU	33	(443) 757-5802